Linear and Nonlinear Barotropic Decay on the Sphere

ISAAC M. HELD AND PETER J. PHILLIPS

Geophysical Fluid Dynamics Laboratory/NOAA, Princeton, NJ 08542

(Manuscript received 5 May 1986, in final form 18 August 1986)

ABSTRACT

An example of the barotropic decay of a wavelike midlatitude disturbance in the presence of a shear flow on the sphere is examined. The linear theory for the evolution of the disturbance is first described, with emphasis on the importance of the pseudomomentum spectrum for the resulting drag on the mean flow. After a brief discussion of the ways in which this linear theory can break down, a high-resolution nonlinear numerical model is used to examine the dependence of the mean-flow modification and the qualitative character of the decay on the amplitude of the initial disturbance.

1. Introduction

Irreversible quasi-horizontal mixing in the troposphere resulting from baroclinic instability can usefully be thought of as consisting of two distinct parts (e.g., Edmon et al., 1980; Hoskins, 1983). The mixing at low levels in the storm tracks results from the complex interplay of occlusion and frontal formation, coupled with nonconservative boundary effects. On the other hand, mixing in the upper troposphere, particularly in the subtropics, results from the breaking of planetary waves that have been excited by these nonlinear instabilities and have propagated vertically and horizontally away from their source regions (cf. the study of an eddy life cycle in the Southern Hemisphere by Randel and Stanford, 1985; the estimates of diffusivity by Plumb and Mahlman, 1986; and the isentropic potential vorticity maps of Hoskins et al., 1985). The simplest possible model in which to analyze the second of these mixing processes is a barotropic model with stirring in midlatitudes to represent baroclinic wave generation. The idea of studying this decay phase of an atmospheric eddy life cycle in isolation can be traced back at least to Kuo (1951).

Using the nondivergent barotropic vorticity equation on the sphere, we examine here some aspects of the linear and nonlinear evolution of a wavelike disturbance initially localized in midlatitudes and superimposed on an idealized zonal flow resembling that found in the upper troposphere. We focus on the drag exerted in the subtropics as a result of the wave dispersion and decay, as it is the competition between this drag and the acceleration by the Hadley cell that determines the structure of the climatological zonal flow in the subtropical upper troposphere. We begin by considering the linear theory for the eddy evolution, highlighting the importance of the pseudomomentum spectrum for the structure of the drag on the zonal flow. We then examine the distribution of the drag as a function of the amplitude of the initial disturbance, hoping to gain some intuition for how the drag is modified as linear theory breaks down.

2. The linear model

Consider the linearized vorticity equation on a sphere of radius a,

$$\tilde{\zeta}_t = -im[a\cos(\theta)]^{-1}(\bar{u}\tilde{\zeta} + \gamma\tilde{\psi}) \tag{1}$$

where $\gamma = a^{-1}\partial_\theta(f + \bar{\zeta})$, m is the zonal wavenumber, and the tilde denotes the complex wave amplitude, $\zeta' = e^{im\lambda}\tilde{\zeta} + (\text{cc})$. The velocity is related to the streamfunction by $\{u, v\} = \{-a^{-1}\partial_\theta\psi, [a\cos(\theta)]^{-1}\partial_\lambda\psi\}$. As an example, we shall consider the stable zonal flow

$$\bar{u} = A\cos(\theta) - B\cos^3(\theta) + C\sin^2(\theta)\cos^6(\theta), \tag{2}$$

with $A = 25$, $B = 30$, and $C = 300$ m s^{-1}, and an $m = 6$ wave with initial meridional structure

$$\tilde{\zeta}(t=0) = (1/2)\zeta_0\cos(\theta)\exp(-[(\theta - \theta_m)/\sigma]^2), \tag{3}$$

with $\theta_m = 45°$ and $\sigma = 10°$. This is the same zonal flow and initial condition as considered in Held (1985). The corresponding zonal mean angular velocity and vorticity gradient profiles are plotted in Fig. 1.

We define the total pseudomomentum P (or "wave activity," see Edmon et al., 1980) and the pseudomomentum density p to be

$$P = \int pa\cos(\theta)d\theta,$$

$$p \equiv \cos(\theta)\gamma^{-1}\overline{\zeta'^2}/2 = \cos(\theta)\gamma^{-1}|\tilde{\zeta}|^2, \tag{4}$$

where an overbar denotes the zonal mean. (Strictly speaking, the pseudomomentum should be defined with the opposite sign, but we prefer to work with a positive definite quantity here.) Here P is conserved in

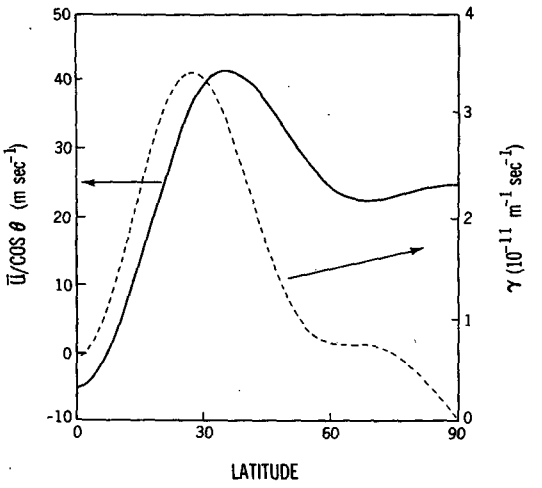

FIG. 1. The zonal mean angular velocity $u/\cos(\theta)$ and the corresponding absolute vorticity gradient used in the linear model and in the initialization of the nonlinear model.

the absence of dissipation. Figure 2a shows the evolution up to day 40 of the pseudomomentum density $p(\theta)$ obtained by numerically integrating (1), after adding to the right-hand side a small amount of linear diffusion, $\nu\nabla^2\zeta$, with $\nu = 10^3$ m^2 s^{-1}. The meridional resolution was decreased until all details of the solution, including the rather complex behavior at high latitudes, were insensitive to the choice of grid size. The density p splits into two parts, the subtropical segment focusing into a fairly narrow latitude band before dissipating. The structure in the polar segment seems to be due to interference between poleward and equatorward propagating waves. (The solution for $\nu = 10^4$ has little of the structure at high latitudes.) The localization of the subtropical segment is essentially completed within $\approx$8 days, after which the disturbance continues to be sheared to smaller meridional scales until the dissipation is intensified. The polar segment continues to evolve in a complex manner beyond the time interval shown.

Since $\partial_t\bar{u} = \overline{v'\zeta'}$ and $\partial_t\overline{\zeta'^2}/2 = -\gamma\overline{v'\zeta'} + \nu\overline{\zeta'\nabla^2\zeta'}$, one has the well-known relation

$$\partial_t\bar{u}\cos(\theta) = -\partial_t p + \nu\gamma^{-1}\cos(\theta)\overline{\zeta'\nabla^2\zeta'},$$

$$\rightarrow [\bar{u}(\infty) - \bar{u}(0)]\cos(\theta) = p(0) + \nu\gamma^{-1}\cos(\theta)\int \overline{\zeta'\nabla^2\zeta'}dt. \tag{5}$$

The zonal mean flow is accelerated in the region of excitation and decelerated where the waves are absorbed. The deceleration obtained from the linear solution [the second term on the rhs of (5)] is also plotted in Fig. 2. We find that 44% of the angular momentum drag is realized poleward and 56% equatorward of the subtropical jet. (One has to integrate for well over a hundred days to obtain a smooth mean flow modification in subpolar latitudes.) The flow is accelerated in midlatitudes by an amount equal to the initial pseudomomentum density, $p(\theta)$. If one thinks of the disturbance as having propagated up from below, then in the absence of dissipation the acceleration in midlatitudes would be balanced by an equal and opposite deceleration that occurs during the upward propagation. The acceleration would be realized at low levels.

As described in Held (1985), P (unlike eddy energy or enstrophy) can be decomposed into contributions from the separate modes of the shear flow:

$$P = \sum P_n + \int \hat{P}(\Omega)d\Omega, \tag{6}$$

where the sum represents the discrete, and the integral the continuous spectrum. The integral ranges from the minimum to the maximum mean flow angular velocity Ω. As shown in Fig. 3 of Held (1985), the excitation of the discrete modes is negligible for a wavenumber 6 initial disturbance with the structure (3) on the flow (2). An estimate of the continuous pseudomomentum spectrum $\hat{P}(\Omega)$ for this disturbance is shown by the histogram in Fig. 3. This result was obtained by finite differencing the eigenvalue problem for modes on this flow, thereby discretizing the spectrum, computing the pseudomomentum projected onto each mode, and then summing up the pseudomomentum in all modes with phase speeds in each of the intervals shown. The result shown was obtained by solving the eigenvalue problem with 90 points from pole to equator; experimenting with different resolutions, we find that some of the details in Fig. 3 are sensitive to this resolution,

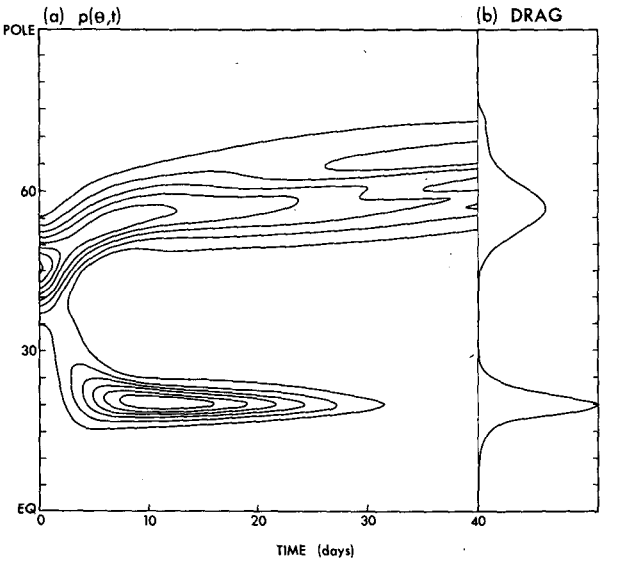

FIG. 2. The evolution of the pseudomomentum density $p(\theta, t)$ (left) and the final zonal flow deceleration (right) obtained from the integration of (1) with small linear diffusion added. The latter is computed from the final term in (5).

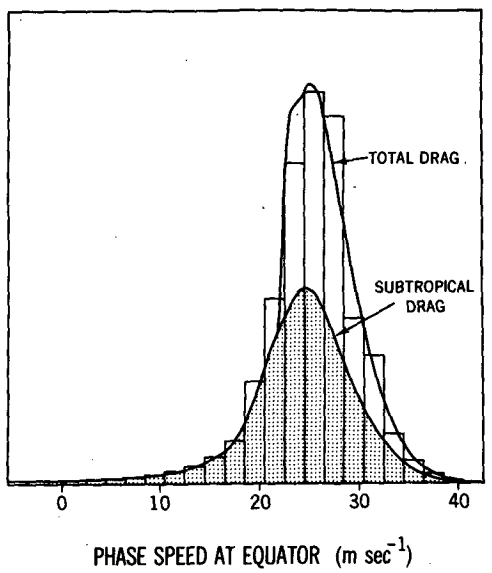

FIG. 3. The pseudomomentum spectrum $P(\Omega)$ as a function of angular phase speed Ω, or equivalently, as a function of the linear phase speed at the equator, Ωa, accumulated in 2 m s^{-1} intervals. Superimposed is the mean flow deceleration in the linear model as a function of zonal mean angular velocity. The shaded region corresponds to the part of this drag deposited equatorward of the jet.

but the basic structure of the spectrum is not. We denote the value of the phase speed at which the spectrum is centered as Ω_0, and the spectral half-width as Δ_Ω. This spectral half-width is inversely proportional to σ, the meridional scale of the initial vorticity disturbance.

Consider that part of the initial condition that projects onto modes with phase speeds between Ω and $\Omega + \delta\Omega$. (One can picture this part of the disturbance as a wavepacket with the meridional wavelength that yields the phase speed Ω, but, in fact, one need not assume that the mean flow is slowly varying in θ.) The inviscid evolution of this part of the disturbance is then given by

$$\tilde{\zeta}(\theta, t) = \int \rho(\Omega)\Phi(\Omega, \theta)e^{-im\Omega t}d\Omega \qquad (7)$$

where $\Phi(\Omega, \theta)$ is the eigenfunction and $\rho(\Omega)$ is nonzero only within the interval $(\Omega, \Omega + \delta\Omega)$. As $t \to \infty$, this integral vanishes at all latitudes θ for which the integrand is nonsingular, by the Riemann–Lebesgue lemma. Since P is conserved, $\tilde{\zeta}(\theta, t)$ cannot vanish at all latitudes. Indeed, $\Phi(\Omega, \theta)$ is singular at "critical latitudes" θ_c where $\bar{\Omega}(\theta_c) = \Omega$. It follows that as $t \to \infty$, $\tilde{\zeta}(\theta, t)$, and the associated pseudomomentum $\hat{P}(\Omega)d\Omega$, must become confined to the latitude band(s) at which critical latitudes exist for this small phase speed interval. If we suppose that the mean flow has a monotonic angular velocity profile, $\bar{\Omega}(\theta)$, then these critical latitudes are confined to a single band of width $\delta\theta = \delta\Omega|\partial\bar{\Omega}/\partial\theta|^{-1}$ located at the latitude at which $\Omega = \bar{\Omega}(\theta)$. It follows that the pseudomomentum density $p(\theta, t)$ approaches $\hat{P}(\bar{\Omega}(\theta))|\partial\bar{\Omega}/\partial\theta|$ as $t \to \infty$. By a process that might be termed Rossby wave chromatography, the shear flow deposits the pseudomomentum of parts of the disturbance that propagate at different phase speeds at different points in the flow (cf. Dickinson, 1969). More generally, we can say that $\sum p(\theta_i, t = \infty) \times|\partial\bar{\Omega}(\theta_i)/\partial\theta|^{-1} = \hat{P}(\Omega)$, where the sum is over all points θ_i at which $\bar{\Omega}(\theta_i) = \Omega$.

For each value of Ω excited in our sample problem, there is one "critical latitude" on the tropical side of the subtropical jet, and one or more on the polar side. On the tropical side of the jet, the critical latitude θ_0 for the dominant phase speed Ω_0 is $\approx 20°$. At this latitude, the angular velocity gradient is relatively large, and as a result the pseudomomentum is focused into a narrow latitudinal band of half-width $\Delta_\theta \approx \Delta_\Omega \times|\partial\bar{\Omega}(\theta_0)/\partial\theta|^{-1}$. Estimating the spectral half-width Δ_Ω from Fig. 3 and computing the mean angular velocity gradient at 20°, we find $\Delta_\theta \approx 2°$, consistent with the sharp focusing seen in Fig. 2. The angular velocity gradients happen to be quite small in high latitudes for this flow (see Fig. 1), and as a result, the pseudomomentum moving poleward is not focused to the same extent.

Assume now that there is dissipation present, but that it is weak enough so as to be negligible at least until the time that the subtropical localization has taken place (less than 8 days according to Fig. 2). Whatever the precise form of the dissipation, one can conclude that the resulting mean flow deceleration will also be focused in a region of half-width Δ_θ, as seen in Fig. 2. If one takes the mean flow deceleration computed numerically with $\nu = 10^3$ m^2 s^{-1}, and combines the subtropical and subpolar parts to compute the drag as a function of the mean angular velocity, one obtains the solid curve in Fig. 3. The result agrees well with the inviscid pseudomomentum spectrum. The subtropical part of this drag is shown by the shading. If the viscosity were reduced even further, the distribution of the drag would not change appreciably; the pseudomomentum would simply decay more slowly. Similarly, if the ∇^2 diffusion were replaced with sufficiently weak scale-selective mixing of a different form (∇^4 or nonlinear) the drag distribution would remain the same.

Figure 4 is a plot of the eddy vorticity as a function of latitude and longitude generated by the linear model at $t = 6$ days. It shows the small meridional scales associated with the localization of the pseudomomentum in the subtropics. If the resolution of the model becomes inadequate for representation of the vorticity field before the localization has been completed, one expects the equatorward movement of the pseudomomentum to be retarded and the drag to be shifted poleward. We have confirmed this with lower resolution models.

3. Breakdown of the linear solution

This linear solution for the drag distribution is self-consistent if the amplitude of the initial condition is

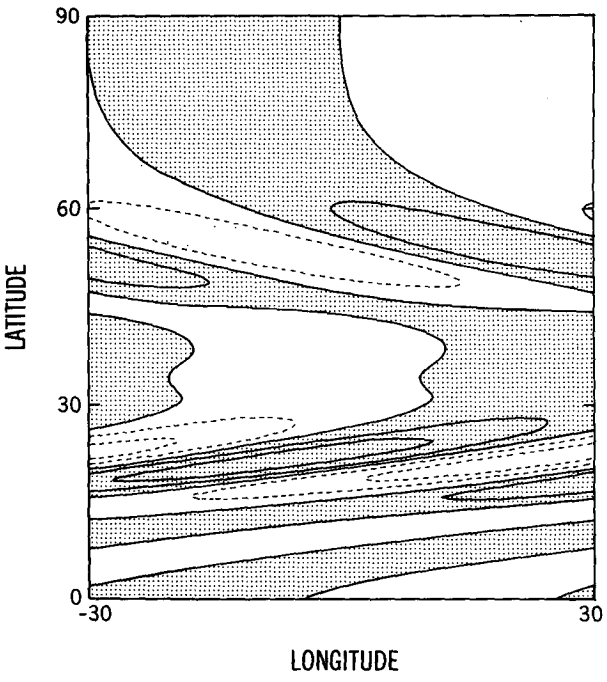

FIG. 4. Eddy vorticity generated by the linear model at $t = 6$ days. Negative values are shaded.

sufficiently small. The following scaling arguments suggest the different ways in which linear theory can break down as the amplitude increases.

Assume for the sake of these scaling arguments that all of the initial pseudomomentum drifts into the subtropics. The pseudomomentum density $p(\theta)$ is initially confined to a band of width σ. As $t \to \infty$, it is focused into a region of half-width $\Delta_y \equiv a\Delta_\theta$ centered at the latitude θ_0. (Δ_y is itself proportional to Δ_Ω, and, therefore, inversely proportional to σ.) Thus, $P \approx \gamma_0 \eta_0^2 \Delta_y$, where $\gamma_0 = \gamma(\theta_0)$ and η_0 is the distance by which particles have been displaced meridionally near θ_0. One criterion for the validity of the linear prediction for the drag on the zonal flow is that η_0 must be smaller than Δ_y; otherwise the drag could not possibly be localized within a region of width Δ_y. This constraint can be rewritten in the form $[P/(\Delta_y \gamma_0)]^{1/2} < \Delta_y$, or

$$P/(\Delta_y^3 \gamma_0) < 1. \tag{8}$$

We estimate that this is the case in our example if $\zeta_0 < 10^{-5}$ s^{-1} in (3).

One obtains the same criterion by requiring that the changes in the zonal mean vorticity gradients be small. The change in the zonal mean wind in the vicinity of θ_0 is $\approx P/\Delta_y$, so the change in the mean vorticity gradient is $\approx P/\Delta_y^3$. If we require that this be smaller than γ_0 we regain (8).

The change in the mean velocity gradient must also be small compared to the original shear, for it is this shear that is stretching the eddy vorticities; therefore, we require $P/\Delta_y^2 < \partial_y \bar{u}$ evaluated at θ_0. If we define a length scale for the initial mean flow as $L \equiv \partial_y \bar{u}/\gamma$ evaluated at θ_0, and set $\xi \equiv L/\Delta_y$, we can rewrite this criterion as $P/(\Delta_y^3 \gamma_0) < \xi$.

A different requirement is obtained from the condition that the eddy velocity gradients be small compared to the mean shear. The induced eddy velocity gradients are of the order of $\zeta_0 \approx \eta_0 \gamma_0 \approx (P\gamma_0/\Delta_y)^{1/2}$, so this condition reduces to $P\gamma_0/\Delta_y < (\partial_y \bar{u})^2$, or

$$P/(\Delta_y^3 \gamma_0) < \xi^2. \tag{9}$$

If this condition is not satisfied, the advection of eddy vorticity by eddy velocities must be taken into account, and the generation of vortices or other coherent structures becomes a possibility. In our example, $\xi \approx 2.5$. Therefore, as the amplitude of the initial condition is increased, we expect the linear prediction for the drag in the subtropics to break down, and the region within which the drag is deposited to widen, somewhat before any tendency develops to generate coherent vortices.

4. Nonlinear integrations

We use a spectral model with rhomboidal truncation at wavenumber 120 to integrate the equation

$$\zeta_t + J(\psi, \zeta) = -\nu \nabla^4 \zeta, \tag{10}$$

with $\nu = 10^{15}$ m^4 s^{-1}, using as the initial condition the disturbance (3) superimposed on the zonal flow (2). We take advantage of the symmetry of the initial condition by retaining only those zonal wavenumbers that are a multiple of 6. Figure 5 shows the globally averaged eddy kinetic energy, normalized by its initial value, as a function of time for different values of the amplitude of the initial disturbance ζ_0. For values of ζ_0 less than 2×10^{-5} s^{-1}, the evolution is nearly independent of amplitude. For larger amplitudes the eddy energy decay follows the linear limit very closely for the first 5 days, but then deviates strongly, as the monotonic decay is replaced by more complex behavior.

In Fig. 6 we plot the change in the zonal mean angular momentum after 15 days of integration, normalized by the squared amplitude of the initial disturbance: $[\bar{u}(t = 15 \text{ days}) - \bar{u}(t = 0)] \cos(\theta)/\zeta_0^2$. We also plot the mean flow modification as $t \to \infty$ predicted by the high resolution linear model (from Fig. 2). The nonlinear model prediction would converge to this linear result as ζ_0 is decreased if the resolution were adequate, if the integration were extended for a sufficient time, and if the dissipation were weaker. The nonlinear result in the subtropics does not change significantly as ζ_0 is decreased below 2×10^{-5} s^{-1}. (We have since found that decreasing the dissipation is sufficient to improve the agreement with the linear model with $\zeta_0 < 2 \times 10^{-5}$.)

The zonal mean absolute vorticity gradient γ at the end of day 15 is plotted in Fig. 7 for several values of ζ_0. In the subtropics, the change in γ is substantial

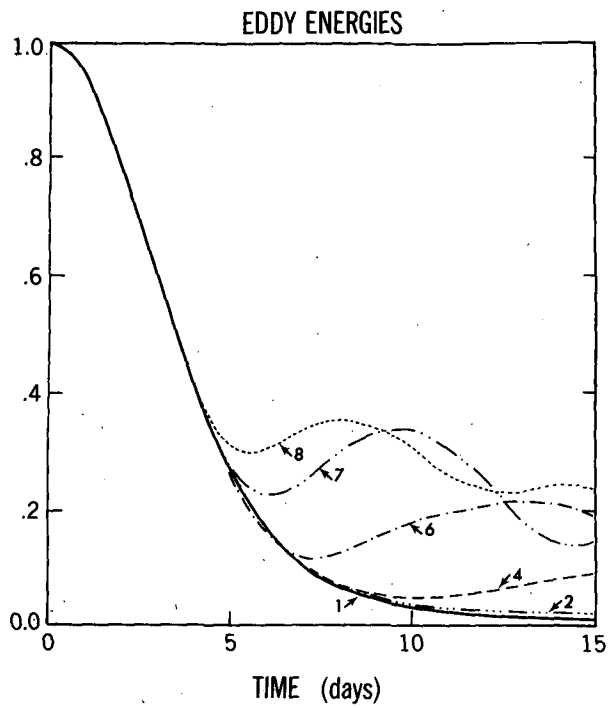

FIG. 5. Global mean eddy kinetic energy normalized by its initial value. The labels refer to ζ_0, the amplitude of the initial disturbance [see Eq. (3)].

once the amplitude of the initial eddy reaches $\zeta_0 \approx 2 \times 10^{-5}$, and the mean vorticity gradient is nearly destroyed at $\approx 25°$ with $\zeta_0 = 4 \times 10^{-5}$. From Figs. 5, 6

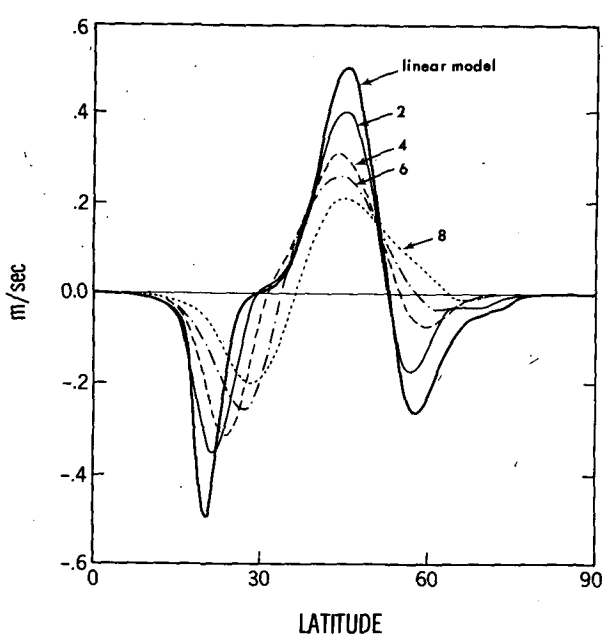

FIG. 6. Mean flow modification for the linear model and after 15 days in the nonlinear model. Labels refer to ζ_0 in units of 10^{-5} s^{-1}. To convert into the unnormalized change in $u \cos(\theta)$, multiply by the label squared.

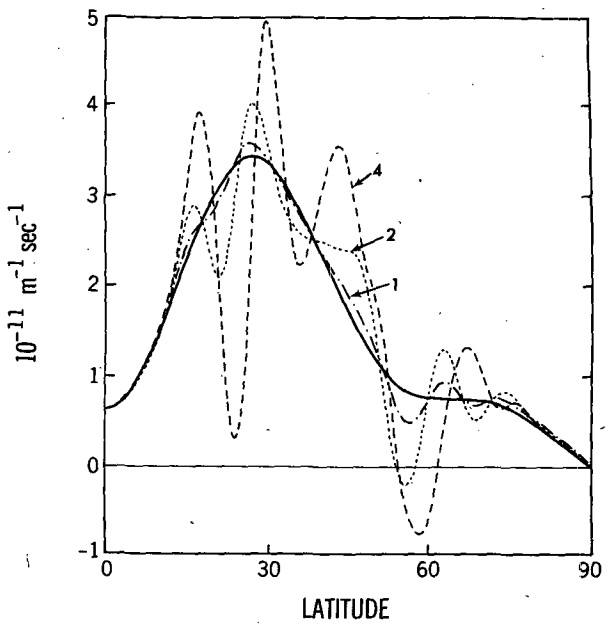

FIG. 7. Zonal mean absolute vorticity gradients at $t = 15$ days. The solid curve is the initial gradient. Labels refer to ζ_0.

and 7 nonlinearity becomes significant in the subtropics for $\zeta_0 > 2 \times 10^{-5}$, consistent with the scaling arguments.

As ζ_0 increases beyond 2×10^{-5}, the structure of the mean flow modification in the subtropics begins to depart significantly from its linear limit; the drag is more broadly distributed and its center is shifted poleward. As discussed in section 3, the broadening of the drag distribution is to be expected as the particle displacements in the subtropics grow in amplitude. The poleward shift is presumably related to the destruction of vorticity gradients near the latitude at which linear theory predicts the greatest mean flow modification, as seen in Fig. 7, thereby preventing the wave from penetrating as far equatorward as the linear theory suggests. Figure 7 also makes clear that nonlinearity becomes important in high latitudes at smaller values of ζ_0 than in the subtropics. In fact, the ratio of the drag deposited in subpolar latitudes to that deposited in the subtropics decreases as ζ_0 increases. This suggests an important limitation of the linear theory, since the ratio of the subpolar to subtropical drag would be an essential element in any eddy flux closure scheme.

Figure 8 contains "snapshots" of the absolute vorticity field at times $t = 0$, 4, 8 and 12 days for the cases $\zeta_0 = 2$ and 4×10^{-5} s^{-1}. Two wavelengths of the disturbance are shown for clarity. In the $\zeta_0 = 2 \times 10^{-5}$ case, the picture is very similar to that obtained by superimposing the linear solution on the initial zonal mean flow. Small scales in the vorticity are created by the impingement of the wavetrain onto its subtropical critical latitude; these are then sheared by the zonal flow, more or less as passive tracers, and eventually lost to dissipation. For the larger amplitude, the evo-

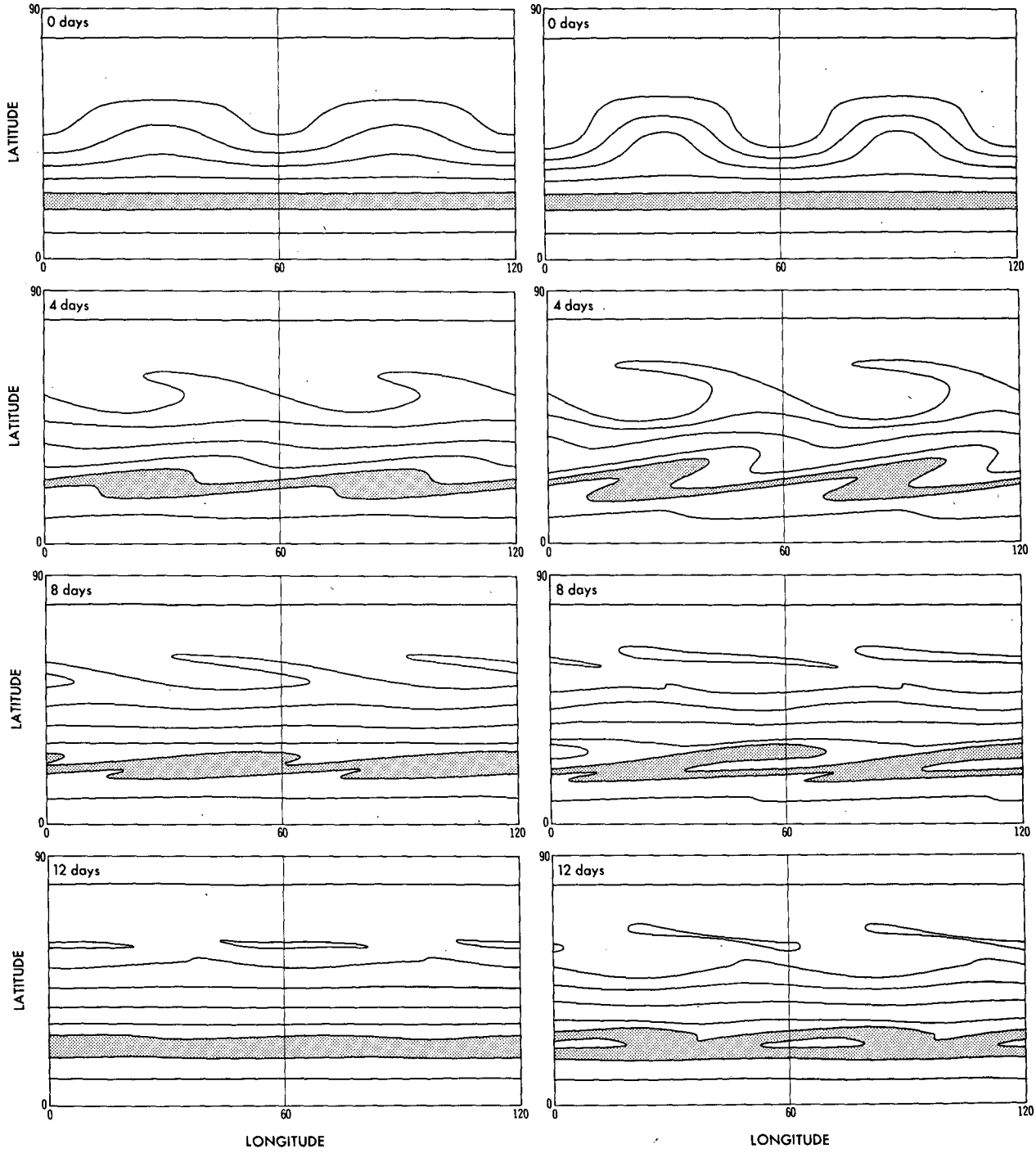

FIG. 8. Absolute vorticity at selected times for the amplitudes $\zeta_0 = 2$ and 4×10^{-5} s^{-1} of the initial disturbance. Two wavelengths of the wavenumber 6 disturbance are shown. The contour interval is 2.0×10^{-5} s^{-1}. Vorticities between 4.0 and 6.0×10^{-5} are shaded.

lution is qualitatively similar but with larger particle displacements in the subtropics. By day 12, isolated patches of vorticity have been created near 25°, but these do not survive more than a few days.

As ζ_0 increases, the particle displacements in the tropics increase further, to the point that long-lived coherent vortices do form. Figure 9 shows the absolute vorticity field for $\zeta_0 = 8 \times 10^{-5}$ at the times $t = 0$, 3, 6, 9, 12 and 24 days. Values of $f + \zeta$ between 3 and 5 $\times 10^{-5}$ are shaded. By day 3, parts of the shaded region have been transported poleward more than 20°. By day 6 the dissipation has cut the filament connecting

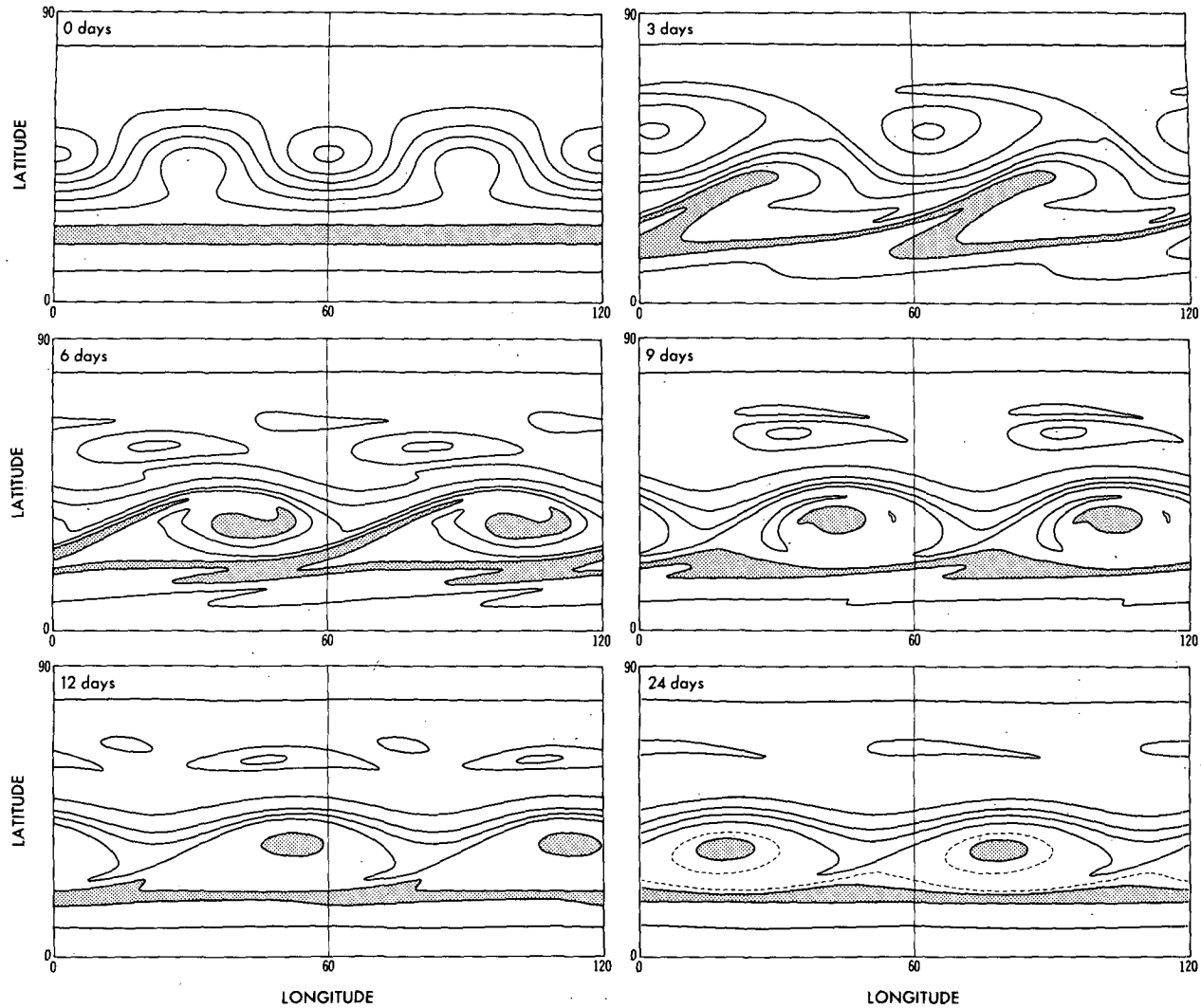

FIG. 9. Absolute vorticity at selected times for an initial amplitude of $\zeta_0 = 8 \times 10^{-5}$ s^{-1}. The contour interval is as in Fig. 8. An extra contour has been added to the figure for day 24.

a large mass of this low vorticity air to its tropical source, and this mass continues to roll up onto itself and mix in a complex manner. By day 12, a well-defined coherent anticyclonic vortex has formed that persists with little change to day 24 and beyond. (In the plot for day 24, we have added a dashed contour to better illustrate the scale of the vortex.) This vortex moves with approximately the same speed as the initial disturbance (as determined from the peak in the pseudomomentum spectrum) which places its critical latitude on the modified mean flow near 32°. The zonal mean absolute vorticity gradient is weakly negative between ~25° and 32° in this state, and the vortex appears to be trapped meridionally between this region of weak vorticity gradient and the strengthened westerlies to the north. If we compute the streamfunction in a frame of reference moving with the corresponding angular velocity, we find a pattern in the subtropics almost identical to that in $f + \zeta$.

In summary, as the amplitude of the initial wave is increased, linear theory first breaks down in the subtropics as meridional particle displacements become larger than the meridional width of the predicted drag distribution. At about the same amplitude, modifications to the zonal mean absolute vorticity gradient become large. At a somewhat larger amplitude, coherent vortices make their appearance, more or less consistent with the scaling arguments in section 3. It should be noted that the mean flow modification is not dramatically altered when large coherent vortices are formed; the broadening of the drag distribution in Fig. 6 for $\zeta_0 = 8 \times 10^{-5}$ is qualitatively what one would expect, based on the lower amplitude cases. While some of the displaced particles have managed to encapsulate them-

selves in protective envelopes which delay their ultimate incorporation into the environmental flow, little meridional mixing of vorticity occurs after the formation of these structures; what mixing there is consists of wisps of vorticity being wrapped around the anticyclones.

We have also performed a number of nonlinear integrations with lower resolution models. A model with rhomboidal truncation at wavenumber 30 (with $\nu = 10^{16}$ m^4 s^{-1}) produces mean flow modifications similar to those of the model described above and also generates coherent vortices at roughly the same wave amplitudes. These vortices have a rather jagged appearance and do not persist as long. A model with rhomboidal truncation at wavenumber 15 shows no sign of coherent vortices.

An initial condition with a full zonal spectrum, as opposed to the sixfold symmetry in these calculations, would undoubtedly produce qualitatively different evolution when the flow is strongly nonlinear. However, the discussion in section 3 makes no reference to the zonal spectrum of the disturbance, implying that the range of validity of the linear prediction for the subtropical mean flow modification could still be estimated from the initial pseudomomentum spectrum.

5. Comments

Can linear theory be used as a basis for a parameterization of the drag due to Rossby wave breaking in the subtropical upper troposphere? Suppose bursts of midlatitude instability are followed by dispersion and decay of the sort modeled in this paper. For the linear prediction of the zonal mean flow modification to be quantitatively valid in our calculation, the initial vorticity has to be less than ≈ 1–2 ($\times 10^{-5}$ s^{-1}), smaller than the vorticities typically present in the midlatitude flow. If we take an amplitude of 2×10^{-5}, assume that the time between bursts is 5 days, and assume that the vorticity in the first disturbance has been sheared to dynamically insignificant scales by the time the next disturbance enters the subtropics so that we can ignore interaction between bursts, the linear theory will predict a drag of $\approx$(0.4 m s^{-1})/day. This is a factor of five or so smaller than the observed upper tropospheric momentum flux convergence (or relative vorticity flux) of ~ 2 m s^{-1}/day in the subtropics (see Lau et al., 1981, p. 80). For bursts every 5 days large enough to generate the observed flux [i.e., with $\zeta_0 \approx 4$–5 ($\times 10^{-5}$)] the linear theory predicts a drag distribution that is too sharp and centered too far equatorward.

The linear prediction would be more accurate for larger amplitude eddies if the spectral width of the disturbance were wider, so that the eddy pseudomomentum would be deposited over a larger span of latitude. It would be of interest to examine the spectral width of observed bursts of eddy activity in the troposphere for this reason.

To generate a drag larger than $\sim 2 \times 10^{-5}$ m s^{-2}, the excitation every 5 days of a disturbance capable of generating large coherent vortices would be required, given the structure of the disturbance we have assumed. While one such burst does not produce qualitatively different drag from smaller amplitude disturbances, if another disturbance is introduced into the flow after the subtropical vortices have been generated, one can easily imagine that the mixing by this new disturbance would be completely modified by the preexisting vortices. In fact, the resemblance of these vortices to the flow in a nonlinear critical layer suggests that the next disturbance would be significantly reflected. However, it is difficult to discuss the effects of successive burst of wave activity without simultaneously modeling the manner in which the resulting zonal mean drag is balanced by meridional flow in the Hadley cell.

Acknowledgments. The motivation for these calculations grew out of discussions with Prof. Q.-C. Zeng on the decay of waves in sheared flows. One of the authors (I.M.H.) would also like to acknowledge very helpful conversations with W. Young and P. Haynes on aspects of this problem.

REFERENCES

Dickinson, R. E., 1969: Theory of planetary wave–zonal flow interaction. *J. Atmos. Sci.*, **26**, 73–81.

Edmon, H. J., B. J. Hoskins and M. E. McIntyre, 1980: Eliassen–Palm cross-sections for the troposphere. *J. Atmos. Sci.*, **37**, 2600–2616. (See also Corrigendum, 1981, *J. Atmos. Sci.*, **38**, p. 1115.)

Held, I. M., 1985: Pseudomomentum and the orthogonality of modes in shear flows. *J. Atmos. Sci.*, **42**, 2280–2288.

Hoskins, B. J., 1983: Modelling of the transient eddies and their feedback on the mean flow. *Large-Scale Dynamical Processes in the Atmosphere*, B. Hoskins and R. Pearce, Eds. Academic Press, 169–199.

——, M. E. McIntyre and A. W. Robertson, 1985: On the use and significance of isentropic potential vorticity maps. *Quart. J. Roy. Meteor. Soc.*, **111**, 877–946.

Kuo, H. L., 1951: The general circulation and the stability of zonal flow. *Tellus*, **3**, 268–284.

Lau, N.-C., G. H. White and R. L. Jenne, 1981: *Circulation statistics for the extratropical Northern Hemisphere based on NMC analyses.* NCAR Tech. Note NCAR/TN-171+STR, 138 pp.

Plumb, R. A., and J. D. Mahlman, 1986: The zonally-averaged transport characteristics of the GFDL General Circulation/Transport model. Submitted to *J. Atmos. Sci.*

Randel, W. J., and J. L. Stanford, 1985: The observed life-cycle of a baroclinic instability. *J. Atmos. Sci.*, **42**, 1364–1373.